Contrasted fate of zinc sulfide nanoparticles in soil revealed by a combination of X-ray absorption spectroscopy, diffusive gradient in thin films and isotope tracing

Maureen Le Bars, Samuel Legros, Clément Levard, Claire Chevassus-Rosset, Mélanie Montes, Marie Tella, Daniel Borschneck, Abel Guihou, Bernard Angeletti, Emmanuel Doelsch

Contrasted fate of zinc sulfide nanoparticles in soil revealed by a combination of X-ray absorption spectroscopy, diffusive gradient in thin films and isotope tracing

Maureen Le Bars [a, ,b, 1], Samuel Legros [c], Clément Levard [a], Claire Chevassus-Rosset [b], Mélanie Montes [b], Marie Tella [d], Daniel Borschneck [a], Abel Guihou [a], Bernard Angeletti [a], Emmanuel Doelsch [b]*

[a] Aix Marseille Univ, CNRS, IRD, INRAE, Coll France, CEREGE, Aix-en-Provence, France

[b] UPR Recyclage et Risque, CIRAD, F-34398 Montpellier, France; Recyclage et Risque, Univ. Montpellier, CIRAD, Montpellier, France

[c] UPR Recyclage et Risque, CIRAD, 18524 Dakar, Senegal; Recyclage et Risque, Univ. Montpellier, CIRAD, Montpellier, France

[d] CIRAD, US Analyse, F-34398 Montpellier, France. Analyse, Univ Montpellier, CIRAD, Montpellier, France

*Corresponding author : maureen.lebars@usys.ethz.ch

Abstract

Incidental zinc sulfide nanoparticles (nano-ZnS) are spread on soils through organic waste (OW) recycling. Here we performed soil incubations with synthetic nano-ZnS (3 nm crystallite size), representative of the form found in OW. We used an original set of techniques to reveal the fate of nano-ZnS in two soils with different properties. ^{68}Zn tracing and nano-DGT were combined during soil incubation to discriminate the available natural Zn from the soil, and the available Zn from the dissolved nano-^{68}ZnS. This combination was crucial to highlight the dissolution of nano-^{68}ZnS as of the third day of incubation. Based on the extended X-ray absorption fine structure, we revealed faster dissolution of nano-ZnS in clayey soil (82% within 1 month) than in sandy soil (2% within 1 month). However, the nano-DGT results showed limited availability of Zn released by nano-ZnS dissolution after 1 month in the clayey soil compared with the sandy soil. These results highlighted: (i) the key role of soil properties for nano-ZnS fate, and (ii) fast dissolution of nano-ZnS in clayey soil. Finally, the higher availability of Zn in the sandy soil despite the lower nano-ZnS dissolution rate is counterintuitive. This study demonstrated that, in addition to nanoparticle dissolution, it is also essential to take the availability of released ions into account when studying the fate of nanoparticles in soil.

[1] Present address: Institute of Biogeochemistry and Pollutant Dynamics, CHN, ETH Zurich, 8092 Zurich, Switzerland

Keywords

Dissolution, availability, clay, sand, speciation

Introduction

Incidental nanoparticles (NPs) are unintentionally formed as a consequence of human activities. We recently illustrated this phenomenon by showing that nanosized zinc sulfide compounds (nano-ZnS) are systematically formed in organic waste (OW) during anaerobic digestion or in liquid OW during storage, thereby boosting nano-ZnS concentrations to up to 1240 $mg_{Zn}.kg_{OW}^{-1}$.[1] Zn is present in high quantities in OW regardless of the origin: urban, industrial or agricultural (40-4000 $mg.kg^{-1}$).[2–6] Nano-ZnS are incidentally spread on soils when OW are applied as fertilizer on cropland. Considering the high Zn concentrations in OW, incidental nano-ZnS are released to a substantially greater extent in soils via agricultural recycling than engineered nano-ZnO, for example (predicted concentration in sewage sludge of about 20 $mg.kg^{-1}$ in Europe, US and Switzerland[7]). Nano-ZnS is also a product of nano-ZnO sulfidation during OW anaerobic treatment.[8,9] However, the environmental fate of nano-ZnS has been little investigated compared to pristine nano-ZnO, which has been extensively studied over the last 10 years.[10–12] Nano-ZnS is a good example of high incidental NP release in the environment that would warrant environmental risk assessment.[13]

Only a few studies have focused on nano-ZnS toxicity in soil.[14–16] Oleszczuk *et al*. (2019)[14] documented the toxicity of around 15 nm ZnS generated by nano-ZnO sulfidation. At 250 $mg_{Zn}.kg_{OW}^{-1}$, nano- ZnS induced 20% *Folsomia candida* mortality and reproduction inhibition in OW-amended soil. Some authors have reported that NP ecotoxicity correlates with the amount of ions released from NP dissolution (e.g. Ag, ZnO).[11,12,17] Zn-based NP dissolution causes the release of free Zn^{2+} ions that are potentially bioavailable, i.e. freely available to cross an organism's cellular membrane.[18] This fraction can have toxic effects when taken up by living organisms.

NPs are considered to be less chemically stable (i.e. dissolve more quickly) than their bulk homologues due to their small size.[19,20] Nano-ZnS incidentally formed in OW are smaller (3-5 nm[1,21–23]) than the 15 nm nano-ZnS studied by Oleszczuk *et al.* (2019).[14] Their toxicity due to Zn release by NP dissolution could therefore be higher. Findings published so far have shown that nano-ZnS formed in OW dissolve within 2 to 6 months in OW or soil,[1,8,23] but the kinetics of this process at the day scale has been overlooked and needs further investigation.

Besides the nanoparticle size, soil properties can also influence nano-ZnS dissolution and released Zn availability. Voegelin *et al.* (2011)[24] revealed different nano-ZnS dissolution kinetics for four soils with different pH, clay and organic carbon content. Numerous studies have highlighted the capacity of phyllosilicates and iron oxides to sorb Zn in soil,[23,25–29] thereby suggesting that the soil mineralogy can control Zn availability in soils because of the varying affinity with the different mineral surfaces. It would thus be essential to identify the soil properties that could influence nano-ZnS dissolution and released Zn availability so as to better predict the nano-ZnS fate in OW-amended soil.

The objective of this study was to determine how soil properties can influence nano-ZnS dissolution kinetics and released Zn availability in soils. Synthesized nano-ZnS representative of nano-ZnS detected in OW were incubated in two different soils with different properties over a 1 month period. The first soil was a silty-clay soil from the island of Réunion (Nitisol) while the second was a sandy-loamy soil from Senegal (Arenosol). We used ^{68}Zn-labelled nano-ZnS to discriminate natural Zn from soil and Zn from nano-ZnS while applying a realistic nano-ZnS input rate (10 $mg_{Zn}.kg_{soil}^{-1}$). During this incubation, the availability of ^{68}Zn released by nano-^{68}ZnS dissolution was evaluated over a time course by measuring the isotopic composition of Zn accumulated on nano-DGT resin (diffusive gradients in thin films [DGT] with 3 kDa dialysis membrane). Then a second incubation with 200 $mg_{Zn}.kg_{soil}^{-1}$ applied nano-ZnS was carried out to determine Zn speciation changes by X-ray absorption spectroscopy (XAS) after 1 month incubation.

Materials and Methods

Soils

Two soils with different properties were selected for this study (Table 1). Nitisol is a silty-clay soil that was sampled in the 0-20 cm layer at La Mare on the tropical volcanic island of Réunion. Arenosol is a sandy-loamy soil that was sampled in the 0-20 cm layer at Sangalkam (30 km west of Dakar) in Senegal. The sampling procedure has been described previously in Doelsch et al. (2010).[30] The soils were analyzed according to the methods described in the supporting data, part I. The mineralogy of both soils was characterized by X-ray diffraction (XRD) after grinding. XRD was performed on a Panalytical X'Pert Pro MPD X-ray diffractometer, with cobalt Kα radiation (λ=1.79Å) at 40 kV and 40 mA. An X'Celerator detector was used (a counting time of 5 s per 0.033° step was used for the 2θ 5-75° range).

Incubation experiment for *in situ* monitoring of Zn availability

The first experiment was designed to determine Zn availability subsequent to release by nano-^{68}ZnS dissolution in soils over a time course during a 1 month incubation experiment.

^{68}Zn (18.75% naturally abundant) was chosen to synthesize labelled nano-ZnS. Zn oxide enriched in ^{68}Zn (99.16%), i.e. ^{68}ZnO, was purchased from Isoflex. ^{68}ZnO was dissolved at 35 mM concentration in HCl (0.1 M). NaOH was added to this solution to increase its pH from 1.2 to 5.1. Nano-^{68}ZnS was synthesized by mixing two solutions of dissolved ^{68}Zn and Na_2S. Initial Zn and S concentrations were selected to have an initial S/Zn molar ratio of 0.9 and a final ZnS concentration of 0.014 M. The pH was 3.6 after mixing the two solutions. After 5 days of rotative agitation in the dark, the suspension was dialyzed (MWCO = 1 kDa) against ultrapure water to remove excess Na^+ and Cl^- ions. Finally, synthesized nano-^{68}ZnS were freeze-dried and ground for XRD characterization and incubation experiments. XRD was performed on a Panalytical X'Pert Pro MPD, X-ray diffractometer, with cobalt Kα radiation (λ=1.79Å) at 40 kV and 40 mA. An X'Celerator detector was used with a counting time of 1400 s per 0.0334° step for the 2 θ 20–75° range. The X-ray diffractogram is shown in Figure S1. The

crystallite size of synthesized nano-^{68}ZnS determined on the (220) peak according to the Scherrer equation was 2.8 nm.[31]

To study the nano-ZnS transformation on a day scale, an incubation experiment was carried out in controlled conditions using the two selected soils, according to the incubation set-up applied in Tella et al. (2016).[32] The soils were incubated for 28 days, in line with other soil and OW incubation studies focused on heavy metals issues.[30,33–35] Nano-^{68}ZnS was added to soil according to actual fertilizing practice (OW spreading rate: 0.01 $kg_{OW}.kg_{soil}^{-1}$) and considering OW with 1000 $mg.kg_{OW}^{-1}$ of Zn as nano-ZnS. A corresponding amount of nano-^{68}ZnS (10 $mg_{Zn}.kg_{DM\ soil}^{-1}$) was mixed with dried soil (40°C) using a powder mixer (Turbula ® T2F T10B). The mixed soil was distributed into cylindric PVC microcosms with an internal diameter of 4.4 cm (30 g $_{DM\ soil}$/microcosm) containing a nano-DGT (R-LSLM, DGT Research LTD) with four replicates per condition. Soils were packed to reach a density of 1.3 $g.cm^{-3}$ and 2.1 $g.cm^{-3}$ for the Nitisol and Arenosol, respectively, which were close measured field densities. Ultrapure water was added to reach a water content of 66% of the maximum water holding capacity (WHC) of the soil. Microcosms were incubated in a closed thermostatic chamber at 28 +/- 1 °C with the soil humidity adjustment weekly. Control soils without nano-^{68}ZnS were treated similarly.

The diffusive gradients in thin films (DGT) measurement provides a calculated Zn concentration representing the diffusion limited, time averaged labile Zn concentrations in the soil. The Zn mass accumulated on DGT resin is correlated with the Zn availability in the soil solution.[36] DGT devices have previously been used to quantify a labile form of a range of metals and nutrients in soils.[37–393] DGT measurement includes Zn resupplied from the solid phase in response to the disequilibrium caused by depletion of the labile Zn pool at the surface of the device.[40] Specific nano-DGT devices were used in this study (LSLM-NP from DGT Research Ltd, UK). Their three kDa dialysis membranes mounted in front of the diffusive gel prevent nanoparticle diffusion.[41,42] The nano-DGT devices were placed in the microcosm at the beginning of the incubation before soil packing and humidification. After 1, 3, 7, 14 and 28 days incubation, the resin layer of nano-DGT devices in contact with soil was retrieved with plastic tweezers and eluted in 1 mL of 1 M ultra-pure HNO_3 (Normatom®; VWR Chemicals), in a closed Eppendorf tube for 24 h at 20°C. The eluate was then diluted in a 2% HNO_3 solution for isotopic ratio measurement. In a previous study with the same incubation set-up and the same Nitisol, it was shown that the binding capacity of the DGT binding layer was not saturated after 90 days of incubation.[32]

The Zn isotope composition of the nano-DGT eluates was measured with a ICP-MS Nexion 300x (Perkin Elmer) in reaction mode, using helium (0.2 $mL.min^{-1}$). From the measured $^{68}Zn/^{66}Zn$ ratio (R_m), we derived the following equations (demonstration can be found in the supporting data, Part III):

1. The $\Delta^{68}Zn/^{66}Zn$ in the nano-DGT eluates:

$$(\Delta^{68}Zn/^{66}Zn)_{DGT} = \frac{R_m}{R_{nat}} - \frac{R_{m_{control\ soil\ at\ t=1day}}}{R_{nat}}$$

R_{nat} is the natural $^{68}Zn/^{66}Zn$ ratio (0.672) verified with a natural Zn solution (Synthetic water EP-L3 (SCP Sciences); [Zn] = 0.0425 mg.kg^{-1}, 6 measurements) and the $R_{control\ soil\ at\ t=1day}$ is the measured $^{68}Zn/^{66}Zn$ ratio in each control soil type after 1 day of incubation. Given that the amount of nano-^{68}ZnS synthesized with the ^{68}Zn spike added to each soil was similar, the $(\Delta^{68}Zn/^{66}Zn)_{DGT}$ traces the amount of Zn released by nano-^{68}ZnS dissolution and accumulated on the DGT resin and enables us to compare the results of the two soils.

2. The mass balance equation to calculate mZn_{sp}/mZn_{tot} ratio:

$$\frac{mZn_{sp}}{mZn_{tot}} = \left[1 + \frac{M(Zn_{nat})}{M(Zn_{sp})} \times \frac{Ab^{66}_{sp}}{Ab^{66}_{nat}} \times \frac{R_m - R_{sp}}{R_{nat} - R_m}\right]^{-1} \text{ and hence } \frac{mZn_{nat}}{mZn_{tot}} = 1 - \frac{mZn_{sp}}{mZn_{tot}}$$

mZn_{sp} and mZn_{tot} are the mass of Zn accumulated on the nano-DGT resin, derived from the spike (i.e. ^{68}Zn solution used to synthesize the nano-^{68}ZnS) and total Zn (natural Zn and Zn derived from the spike), respectively. R_{sp} is the $^{68}Zn/^{66}Zn$ ratio in the spike (R_{sp} = 619.8 from the the Isoflex ^{68}ZnO certificate). $M(Zn_{sp})$ and $M(Zn_{nat})$ are the molar masses (g.mol^{-1}) of Zn used to synthesize nano-^{68}ZnS and natural Zn, respectively. Ab^{66}_{nat} and Ab^{66}_{sp} represent the abundance of ^{66}Zn isotopes in natural zinc and spiked zinc, respectively. Errors on $\Delta^{68}Zn/^{66}Zn$ and mZn_{sp}/mZn_{tot} were estimated lower than 20% and 5%, respectively. The analytical methods are described in further detail in the supporting data, part III.

After retrieving the nano-DGT resin, 1 g of soil was used for microbial activity determination (supporting data, part IV) and soil pore water was extracted for pH measurement (supporting data, part V).

Statistical tests were performed with XLSTAT software to compare $(\Delta^{68}Zn/^{66}Zn)_{DGT}$. A Kruskal-Wallis test (5% significance) was used for the comparison of the samples (n=10) according to one parameter ($(\Delta^{68}Zn/^{66}Zn)_{DGT}$). The four values obtained from the four replicates were considered for this comparison. In case of rejection of the null hypothesis (H0 = all samples from the same population), a Conover-Iman post-hoc test was used for multiple pair-wise comparison with Bonferroni correction. The p-values obtained were compared to the corrected Bonferroni significance levels (0.0011) to determine significant differences.

Incubation experiment for characterization of Zn speciation

A second experiment was carried out to determine Zn speciation after 1 month incubation using the selected soils amended with nano-ZnS.

Nano-ZnS were synthesized by mixing $ZnCl_2$ and Na_2S solutions to reach a final ZnS concentration of 0.04 M with a molar ratio S/Zn of 0.5. The suspension pH after mixing was 3.6. After 10 days of rotative agitation in the dark, the suspension was dialyzed (MWCO = 1kDa) against ultrapure water. Finally, synthesized nano-ZnS was freeze-dried and ground for XRD characterization and homogeneous mixing with soil. The XRD parameters were the same as for nano-^{68}ZnS characterization and the X-ray

diffractogram is shown in Figure S2. A crystallite size of 2.5 nm was determined with the Scherrer equation.[31]

10 g of both soils were mixed with nano-ZnS at a concentration of 200 $mg_{Zn}.kg_{DM\ soil}^{-1}$. We opted for this concentration to be able to determine the speciation of exogenous Zn resulting from the nano-ZnS input in the light of the X-ray absorption spectroscopy detection limit and the natural Zn concentration of the Nitisol (170 $mg.kg^{-1}$). Soils mixed with nano-ZnS were packed and humidified in the same conditions as in the first incubation. After 1 month, the soils were freeze-dried and ground for XAS characterization.

Zn K-edge absorption spectra were recorded at the SOLEIL synchrotron (Saclay, France) on the SAMBA beamline. Each spectrum was measured at 10-15 K to prevent sample beam damage. Spectra were measured in fluorescence mode with a Canberra 35-element Ge detector. The spectra were an average of up to 40 scans, depending on noise level. Energy calibration was performed using a metallic Zn reference foil (absorption edge defined at 9659 eV). Normalization and data reduction were performed using Athena software.[43]

Least square linear combination fitting (LCF) was performed for each soil spectrum over a k-range of 2.5 - 10.6 $Å^{-1}$ using Athena software. The library of Zn reference compounds, used to identify Zn species in soils, included reference compounds described elsewhere[1,22,32,44–47] (Amorphous Zn-phosphate, commercial ZnS, Zn-cysteine, Zn-histidine, Zn-malate, Zn-sorbed to ferrihydrite (Zn-FeOx), Zn-methionine, Zn-cryptomelane, Zn-phosphate, Zn-phytate, Zn-goethite, Zn-oxalate-hydrate, sphalerite, smithsonite, zincite and Zn hydroxide). The quality of the LCF was evaluated using the residual factor $R = \Sigma(k^3\chi(k)_{exp} - k^3\chi(k)_{fit})^2/\Sigma(k^3\chi(k)_{exp})^2$. At each step of the fitting, an additional reference spectrum was added if the two conditions were fulfilled: the R factor decreased by 20% or more and the additional reference had a contribution equal to or higher than 10% among Zn species. The uncertainty of this LCF method was estimated at +/- 15%. The sum of fitted fractions (96 and 109% respectively for the Nitisol and Arenosol) were normalized to 100 % for comparison.

Results and Discussion

Increased Zn availability in the Arenosol exposed to nano-^{68}ZnS

The $(\Delta^{68}Zn/^{66}Zn)_{DGT}$ was significantly higher in soils exposed to nano-^{68}ZnS than in the control soils, since the third day of exposure in both soils (Figure 1 a, b) and throughout the incubation period. This difference indicated that a significant fraction of ^{68}Zn accumulated in the nano-DGT resin originated from nano-^{68}ZnS dissolution, regardless of the soil type. The time-course pattern was similar for the two soils: there was a rapid increase of the $(\Delta^{68}Zn/^{66}Zn)_{DGT}$ during the three first days of incubation and a second phase characterized by a slight increase.

The same nano-^{68}ZnS mass was applied to both soils, representing 6 and 30% of the total Zn in the Nitisol and Arenosol microcosms, respectively (Figure 2 a). However, ^{68}Zn released by nano-^{68}ZnS dissolution accounted for 50% and 75% of the total Zn accumulated on nano-DGT resin in the Nitisol and Arenosol, respectively (Figure 2 b). This highlights the chemical instability[48] of nano-^{68}ZnS and their higher potential to release available Zn compared to naturally occurring Zn.

The $(\Delta^{68}Zn/^{66}Zn)_{DGT}$ was significantly greater in the Arenosol than in the Nitisol from the third day of incubation (Figure 1 c). The higher $(\Delta^{68}Zn/^{66}Zn)_{DGT}$ noted for the Arenosol compared to that of the Nitisol could be explained by an increased dissolution of applied nano-^{68}ZnS and/or higher availability of released ^{68}Zn.

The difference in the nano-^{68}ZnS chemical stability in these two soils could not be revealed by the $(\Delta^{68}Zn/^{66}Zn)_{DGT}$ alone. Indeed, we could not determine whether the lower $(\Delta^{68}Zn/^{66}Zn)_{DGT}$ for the Nitisol was due to a lower dissolution of nano-^{68}ZnS and/or lower availability of released ^{68}Zn. Extended X-ray absorption fine structure (EXAFS) characterization of soils after nano-ZnS application appeared to be a suitable method for evaluating nano-ZnS stability in soils.

Zn speciation reveals nano-ZnS dissolution in the Nitisol

A significantly different fate of nano-ZnS in the two soils was highlighted by contrasted EXAFS spectra 1 month after nano-ZnS application (Figure 3). The Arenosol + nano-ZnS spectrum was similar to the nano-ZnS reference spectrum with structured oscillations (e.g. 6.5, 7.5 and 9.1 A^{-1}), whereas the Nitisol + nano-ZnS spectrum had smoother oscillations with few structured features similar to the Zn-kaolinite and Zn-iron oxide (Zn-FeOx) reference compounds. Linear combination fitting (LCF) of the Nitisol + nano-ZnS spectrum involved a combination of four references (36% Zn-kaolinite, 39 % Zn-FeOx, 15 % Zn-cryptomelane, 10 % nano-ZnS). At the beginning of the incubation period, 2 mg of Zn as nano-ZnS were applied on the Nitisol, representing 54% of the total zinc in soil (T0 in Figure 4). However, after 1 month incubation, the nano-ZnS fraction only represented 10% of the total zinc. This decrease revealed the dissolution of 1.6 mg of nano-ZnS in the Nitisol, i.e. 82% of the applied nano-ZnS. Conversely, the Arenosol + nano-ZnS spectrum were fitted with nano-ZnS (88%) and Zn bound to an undefined soil compound (12%) after 1 month incubation (using Zn-kaolinite, Zn-phosphate or Zn-iron oxide reference

spectra gave the same quality of fit). Originally, the 2 mg of applied nano-ZnS represented 90% of the total zinc in the Arenosol exposed to nano-ZnS (T0 on Figure 4). The final speciation after 1 month incubation revealed the dissolution of 0.04 mg of Zn as nano-ZnS, i.e. 2% of the nano-ZnS dissolved (Figure 4). This comparison revealed that there was more dissolution of applied nano-ZnS in the Nitisol than in the Arenosol.

The full picture: when nanoparticle dissolution does not mean increased availability in soils

Evidence of fast 3 nm nano-ZnS dissolution

The nano-^{68}ZnS dissolution pattern starting during the third day of soil incubation (Figure 1 a and b), highlighted faster dissolution than has been observed to date. In a previous field study, we had shown that nano-ZnS (~ 3 nm crystallite size), which accounted for 100% of speciation in pig slurry, was not detected in a clayey soil 6 months after pig slurry amendment,[23] but no measurements of Zn speciation in amended soil were performed at shorter times. Here, by combining nano-DGT and ^{68}Zn tracing, we were able to monitor nano-ZnS dissolution at a day scale. Fast nano-ZnS dissolution was detected for both soils, regardless of their properties.

3 nm nano-ZnS dissolved more quickly (e.g. 82 % after 1 month in the Nitisol, Figure 4) compared to larger ZnS particles. Indeed, Voegelin *et al.* (2011)[24] assessed the dissolution of commercial ZnS (25-40 nm) in four different soils. The fastest dissolution rate was observed for a loamy soil in which 76% of nano-ZnS had dissolved within 2 years. For 63 µm sphalerite crystals, dissolution rates in soils were even slower: 0.6 to 1.2% within 1 year.[49] Moreover, in our previous study, we had shown the dissolution of nano-ZnS (3 nm) formed in OW within 2 months of composting.[1] Therefore, the fast dissolution of nano-ZnS of around 3 nm size could be explained by the nanosize of these compounds. Indeed, structural changes induced by the < 20 nm size could affect the NP chemical stability.[19] More specifically, 3.4 nm nano-ZnS exhibited a significant lattice contraction compared to their bulk homologues.[50] Lattice contraction is interpreted as being the result of the hydrostatic pressure exerted by surface stress within a continuum elastic model.[51] We hypothesize that particles with lattice contraction are more reactive than larger particles due to increased surface stress.

Enhancement of nano-ZnS dissolution in clayey soils

After 1 month incubation in the Arenosol, only 2% of 3 nm nano-ZnS compounds were dissolved as compared to 82% observed for the Nitisol. Several assumptions could explain these discrepancies.

First, the mineralogical compositions of the Nitisol and Arenosol sharply contrasted (Figure 5). Quartz mainly accounted for the Arenosol mineralogy whereas the Nitisol contained a more diversified mineralogy with the presence of clays (kaolinite and halloysite), iron and aluminum oxy-hydroxide (magnetite, hematite, goethite, ilmenite and gibbsite). Those minerals have been identified in the literature for their capacity to sorb Zn.[23,25–29] In the case of the Nitisol, our XAS results have shown that Zn released by nano-ZnS dissolution is sorbed on iron oxides (ferrihydrite), clays (kaolinite), and

potassium manganese oxide (cryptomelane). Similarly, Formentini *et al.* (2017)[23] observed that Zn released by 3 nm nano-ZnS dissolution was complexed with organic matter and sorbed to kaolinite and iron oxides. These minerals are thus suspected to have an impact on nano-ZnS dissolution in Nitisol. Indeed, in a simpler system with only nano-ZnS and water, Zn partitioning could reach equilibrium with a given percentage of Zn in water and nano-ZnS. In a more complex soil system, waterborne Zn could be sorbed on other solid surfaces in the soil (the minerals mentioned above). This sorption would decrease the waterborne Zn concentration and induce more nano-ZnS dissolution.[52] Such promoted dissolution was not observed for larger particles: Voegelin *et al.* (2011)[24] observed only ~7% dissolution of 25-40 nm nano-ZnS after 2 years for a clayey soil (47%, including kaolinite). We consider that both the nano-scale and the soil mineralogy could drive the fate of ZnS in soil.

Nano-ZnS dissolution could also have been induced by the ligand competition mechanism in the Nitisol. Indeed, ligand-mediated dissolution has already been reported for several nanoparticles. Siy *et al.* (2010)[53] showed an increase in CdSe NPs dissolution in the presence of organic ligands (stearic acid, oleic acid, octadecylamine). EDTA is a strong complexing agent that enhances Ag-NP dissolution.[54] Moreover, it was shown that CuS or HgS nanoparticles did not dissolve in oxic conditions without natural organic matter.[55–57] For ZnS, according to Zhang *et al.* (2010)[58] based on thermodynamic models, small nano-ZnS compounds cannot dissolve without EDTA complexation in solution at pH 9-10. In the Nitisol, organic ligands were more abundant than in the Arenosol, as shown by the C_{org} content of the two soils (2.3 and 0.76%, respectively (Table 1)). As natural organic matter is known to bind trace metals, including Zn,[59] Zn complexation with organic matter could also have contributed to nano-ZnS dissolution in the Nitisol.

Biotic or abiotic sulfur oxidation could have enhanced nano-ZnS dissolution in the Nitisol. Indeed, ZnS can be dissolved by sulfur oxidation in the presence of O_2[60] or via Fe^{3+} reduction:[61]

$$ZnS + O_2 \rightarrow Zn^{2+} + SO_4^{2-}$$

or

$$ZnS + 8Fe^{3+} + 4H_2O \rightarrow Zn^{2+} + 8Fe^{2+} + SO_4^{2-} + 8H^+$$

Heidel *et al.* (2011)[60] showed that sphalerite dissolution occurred through O_2-induced sulfur oxidation during the first days. Then Fe^{2+} released by sphalerite dissolution was oxidized by O_2 and resulted in sphalerite oxidation by Fe^{3+}. *Thiobacillus ferrooxidans* bacteria were shown to enhance ZnS dissolution by Fe^{2+} oxidation into Fe^{3+} combined with removal of the S^0 layer formed at the ZnS surface, thereby hindering the rate of Fe^{3+} diffusion.[62] Some bacteria like *Acidithiobacillus thiooxidans* can directly oxidize sulfur,[63] but *T. ferrooxidans* and *A. thiooxidans* have not been previously detected in agricultural soils,[64,65] probably because the pH in these soils is not within their optimal pH range (1.3-4.5).[66] Neutrophilic sulfur-oxidizing *Thiobacillus* bacteria have been detected in agricultural soils, including *T.*

thioparus, *T. denitrificans* and/or *T. plumbophilus*.[64,65] In addition, ZnS dissolution could occur in bacterial biofilms that form in soils, as shown by Desmau *et al.* (2020)[67] for CdSe/ZnS quantum dots in *Shewanella oneindensis* biofilms. Our results did not show a significant difference between total bacterial activity in the Nitisol and Arenosol (supporting data, Part IV). However, this does not exclude the possibility that some specific biological activity not detected by the total bacterial activity measurement, such as iron/sulfur oxidation, was higher in the Nitisol than in the Arenosol.

Clayey soil properties limit Zn availability

^{68}Zn released by nano-^{68}ZnS dissolution had a contrasted fate depending on the soil type. As the XAS results revealed faster dissolution in the Nitisol than in the Arenosol, we would expect that more ^{68}Zn accumulated on the nano-DGT resin in the Nitisol, and therefore a higher $(\Delta^{68}Zn/^{66}Zn)_{DGT}$. The fact that the opposite trend was observed suggests that the availability of Zn released by nano-ZnS dissolution was strongly dependent on the soil properties. Indeed, Zn availability depends on its physicochemical affinity for the different soil constituents. In particular, cation exchange reactions, specific adsorption processes, surface precipitation on mineral surfaces or complexation with soil organic matter are possible reactions that have been widely described to affect metal retention in soils.[68] These processes are governed by the pH, which plays a key role in trace element partitioning between solid and solution phases in soil.[69,70] However, at t=28 days, the pH levels were quite similar, i.e. 4.7 and 5.1 for the Nitisol and the Arenosol, respectively (supporting data, Part V). Therefore, we assumed that factors other than pH control Zn availability in these soils. Several authors have argued that Nitisol has a stronger retention capacity than Arenosol.

The cationic exchange capacity (CEC) is an overall indicator of the soil capacity to sorb cations, including Zn^{2+}, through cation exchange reactions. The CECs of the Nitisol and Arenosol were 11.6 and 7.1 cmol.kg^{-1}, respectively. The higher CEC value for the Nitisol could be explained by its higher clay fraction (42.7%) compared to that in the Arenosol (10.2%). Isomorphous substitution of cations in clays causes a pH-independent negative charge favoring cationic adsorption (e.g. Al^{3+} substitutes for Si^{4+} in the tetrahedral sheet causing a negative charge).[71] The clay fraction has been identified as the principal driver of Zn retention in soils based on investigations on the solid/solution partitioning coefficient (K_d) in various conditions and through statistical analysis of large soil datasets.[72]

Specific (pH dependent) adsorption phenomena can also occur. A number of spectroscopic studies have documented the formation of specific inner-sphere complexes on the surface of iron oxides and clays identified in Nitisol (hematite, kaolinite, goethite). Zn was found to bind to hematite through a mononuclear inner-sphere complex at pH 5.5.[73] Nachtegaal and Sparks showed that Zn formed a bi-dentate inner-sphere sorption complex on the goethite surface at pH 5.[74] In the same study, they found that Zn formed a monodentate inner-sphere sorption complex at the kaolinite surface with Zn binding to Al-OH edge groups. Similar results were obtained for Zn sorbed on kaolinite at pH 5.5.[75] In all of the above-cited studies, no surface precipitation was observed, which usually occurs at higher pH and

surface coverage.[74] Conversely, for quartz, the main Arenosol constituent, a combined isotopic and spectroscopic study revealed that, below pH 7, Zn predominantly formed outer-sphere sorption complexes on the quartz surface.[76] Outer-sphere complexes, contrary to inner-sphere complexes, are reversible.

Complexation with organic matter can also reduce Zn availability in soil as the organic carbon concentration is higher in Nitisol (2.3%) than in Arenosol (0.76%). Indeed, Formentini *et al.* (2017)[23] showed that Zn applied to a clayey soil via pig slurry spreading was no longer present in the initial nano-ZnS form, and 41% of this exogenous Zn was bound to organic molecules. Through a statistical analysis of the findings of over 302 soil studies, Sauvé *et al.* (2000)[70] highlighted that soil organic matter (SOM) was a major factor affecting Zn solid/solution partitioning in soil, where a high SOM content was found to decrease available Zn in soil.[70] Furthermore, several studies have highlighted the formation of inner sphere complexes between Zn and SOM.[77–79]

The tortuosity of the diffusion pathway could also explain a lower diffusion of available ^{68}Zn to nano-DGT resin in Nitisol.[80] Indeed, solute transport in soil is controlled by the soil texture, water content and dry bulk density.[81] Particularly, for a same water content, it was shown that Cl^- diffusivity was favored in sandy soils compared to clayey soils.[82] According to the models developed to predict solute diffusivity,[83,84] the relative solute diffusivity coefficient in Arenosol was estimated to be around 1.5-fold higher than in Nitisol based on their different clay and organic matter content, volumetric water content and dry bulk density (see supporting data, Part VI).

Environmental implications

These results are surprising and could have led to opposite conclusions on the environmental implications if presented independently. Indeed, we were expecting that: (i) high nano-ZnS dissolution would be associated with high Zn availability, and (ii) low nano-ZnS dissolution would be associated with low Zn availability. Indeed, Sekine *et al.* (2015)[41] demonstrated that nano-Ag_2S had high chemical stability in soil (highlighted by XAS) while Ag had a low availability (highlighted with nano-DGT). Combining XAS, nano-DGT and isotope tracing was essential in drawing the key conclusion of this study, i.e. high NP dissolution does not necessarily means high element availability and vice versa.

Our results provide new keys for understanding the fate of Zn in soils. We obtained evidence that, in a clayey soil, most nano-ZnS were dissolved whereas most of the released Zn was quickly immobilized. Nano-ZnS application on such soils would therefore have little impact on Zn availability in the short term. Yet, while nano-ZnS dissolution is much slower in a sandy soil, the released Zn would be more available. Application of nano-ZnS on such soils could thus have a significant impact with respect to Zn availability and toxicity. These results must be complemented by further studies to identify the long-term impact of OW recycling on Zn contamination in soils. The stability of Zn associated with the identified bearing phase in Nitisol (clay, iron oxide, manganese/potassium oxide) should be evaluated

over a longer term under varying climate conditions. Indeed, Tella *et al.* (2016)[32] showed that Zn-FeOx speciation in organic waste was correlated with Zn availability in OW-amended soil. This result was explained by soil acidification following organic matter mineralization, which would induce Zn desorption from iron oxide. This mechanism should be considered with regard to the fate of Zn sorbed on iron oxide in Nitisol. On the other hand, after 11 years of repeated pig slurry amendment, Zn was found to accumulate in the top 30 cm of a clayey soil, and was sorbed on clay, iron oxide and organic matter.[23] These findings suggest that Zn bearing phases and the small granulometry composing the Nitisol would also limit Zn transfer to deeper soil layers in a longer term.

When nano-ZnS are formed in OW, organic matter composing OW can interact with the nano-ZnS surface. Likewise, OW-borne nano-ZnS are potentially biogenic due to the presence of sulfate-reducing bacteria,[13] and could therefore be closely associated with extracellular proteins[85] that in turn could change the nano-ZnS properties. Indeed, it was shown that organic molecules with a thiol group had an influence on nano-ZnS aggregation properties.[86,87] It is also possible that these molecules influence the size and structure properties, as water molecule surface interactions with 3 nm nano-ZnS can increase their crystallinity.[88] According to the mechanisms highlighted by our study, systems with higher complexity should now be studied, e.g. the fate of nano-ZnS in soils, using nano-ZnS precipitated in the presence of organic matter or directly precipitated in OW. Organic matter application by OW recycling on soils can alter the physicochemical conditions in soil (e.g. pH variation due to organic compound mineralization[32]), thereby changing the Zn adsorption behavior and fate. Furthermore, the presence of plants in the soil is expected to influence the nano-ZnS fate. Indeed, Panfili et al. (2015)[89] showed that a higher proportion of ZnS was detected in unvegetated sediment (26-49% of total Zn) compared to vegetated sediment (0-11% of total Zn), suggesting that the physicochemical changes due to the presence of plants had induced ZnS dissolution.

Conclusion

In conclusion, a combination of two factors govern the Zn fate in cropland soils, i.e. Zn speciation and soil properties. We previously showed that the OW treatment choice (anaerobic digestion vs. composting) controlled Zn speciation in OW[1] and that Zn speciation in OW was a key factor controlling the environmental fate of this element in OW-amended soils.[90] The present study revealed another key parameter to consider when evaluating environmental impact of OW recycling regarding Zn contamination, i.e. the amended soil properties. Further research is required to identify the parameters controlling nano-ZnS dissolution and released Zn availability. For example, a dissolution study in aqueous solution with a different chemical composition would be of interest to identify the principal factors driving nano-ZnS dissolution in soils. According to our results with these two different soils, several hypotheses could be put forward to explain the faster nano-ZnS dissolution in the Nitisol and the higher availability in the Arenosol: (1) Zn affinity for Nitisol minerals, (2) Zn complexation with

organic molecules (3)(a)biotic sulfur oxidation favored in Nitisol, and (4) higher Zn diffusivity in Arenosol.

Conflicts of interest

There are no conflicts to declare.

Acknowledgment

We are grateful to the French Environment and Energy Management Agency (ADEME) and the French Agricultural Research Centre for International Development (CIRAD) for funding the PhD scholarship of Maureen Le Bars. This study was part of the DIGESTATE project, funded by the French National Research Agency (ANR) under Grant ANR-15-CE34-0003-01. We acknowledge SOLEIL for provision of synchrotron radiation facilities and we would like to thank Gautier Landrot for assistance in using the SAMBA beamline. We wish to thank the CIRAD Laboratory of Water, Soil and Plant Analysis (US Analyses, CIRAD, Montpellier, France) and US Imago-Dakar (IRD) for the laboratory analyses. E. Doelsch received funding from the EU Horizon 2020 Framework Programme for Research and Innovation under the Marie Skodowska-Curie actions agreement N°795614.

Table 1 : Soil properties. Concentrations are expressed on a dry matter (DM) basis.

Parameters		**Nitisol**	**Arenosol**
Granulometric composition	Clay (%)	42.7	10.2
	Silt (%)	46.5	11.5
	Sand (%)	10.8	78.3
[C_{org}] %		2.3	0.76
$[Zn]_{total}$ mg.kg^{-1}		170	19
CEC[1] cmol(+).kg^{-1}		11.6	7.1
pH in water		6.5	6.8
Max WHC[2] (L.kg^{-1})		0.46	0.26

The analytical methods are described in the supporting data, part I.
1. CEC : cation exchange capacity ; 2. WHC : water holding capacity

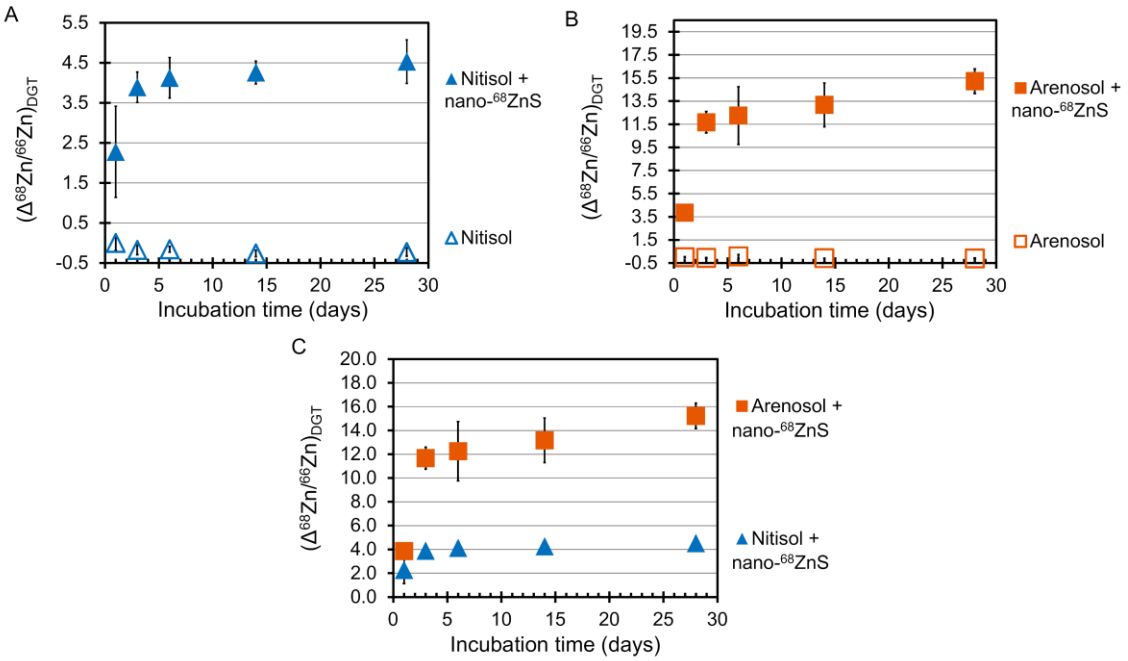

Figure 1 : Isotopic composition of Zn accumulated on nano-DGT resin ($\Delta^{68}Zn/^{66}Zn)_{DGT}$ during soil incubation. Comparison of the Nitisol exposed to nano-^{68}ZnS and the control Nitisol (A), comparison of the Arenosol exposed to nano-^{68}ZnS and the control Arenosol (B) and comparison of the two soils exposed to nano-^{68}ZnS (C). Error bars represent the standard deviation of the four replicates.

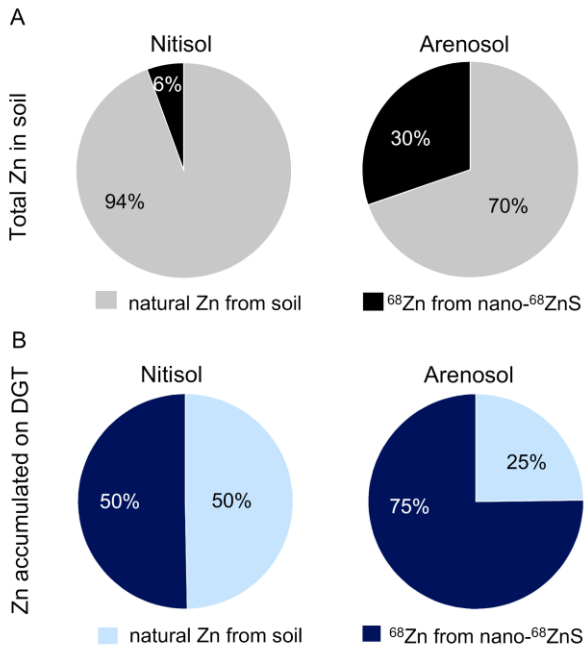

435

436 *Figure 2 : A) Total zinc in the two soils with respective proportion of naturally occuring Zn and ^{68}Zn from nano-*
437 *^{68}ZnS, B) Zinc accumulated on nano-DGT for the two soils with respective proportion of naturally occuring Zn*
438 *and ^{68}Zn from nano-^{68}ZnS (mZn_{nat}/mZn_{tot} and mZn_{sp}/mZn_{tot}).*

439

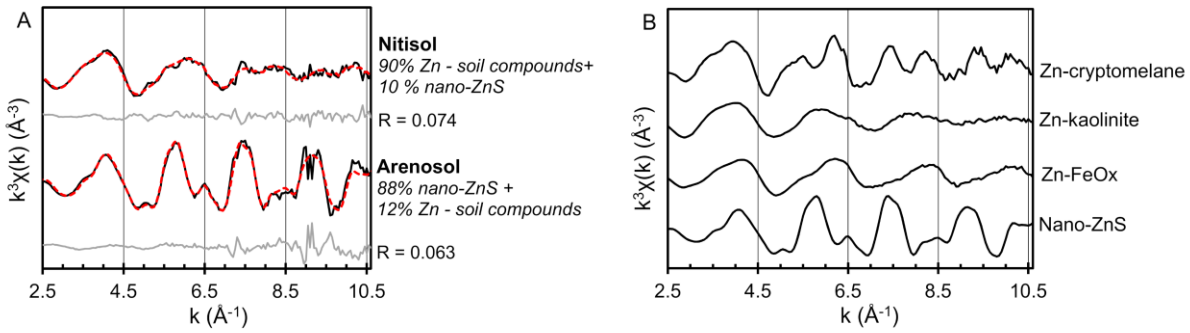

440

441 *Figure 3 : Zn K-edge extended X-ray absorption fine structure spectroscopy of (A) soils spiked with nano-ZnS*
442 *after 1 month incubation (black), best linear combination fitting (red) and fit residue (grey) with R the calculated*
443 *residual factor of the fit. (B) Zn reference compounds selected by linear combination fitting of the soils.*

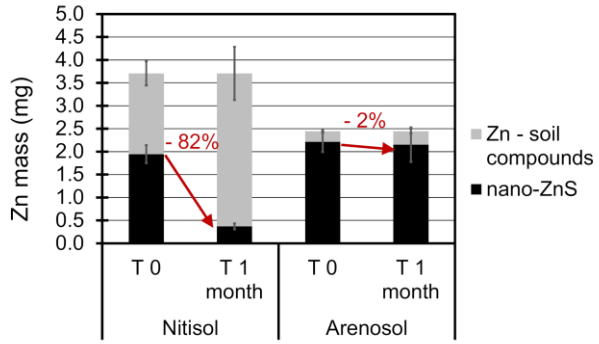

Figure 4 : Zn mass in each soil shown as applied nano-ZnS or Zn bound to soil compounds for both soils at the initial and final incubation times, calculated from the known $[Zn]_{soil}$ and mass of applied nano-ZnS for the initial time, and from the XAS speciation results after 1 month exposure. Error bars include the error of the ICP-MS measurement (15%) and the soil/nano-ZnS weighting (0.1 mg) for T0 and T1 month, and LCF error (15%) for T 1 month.

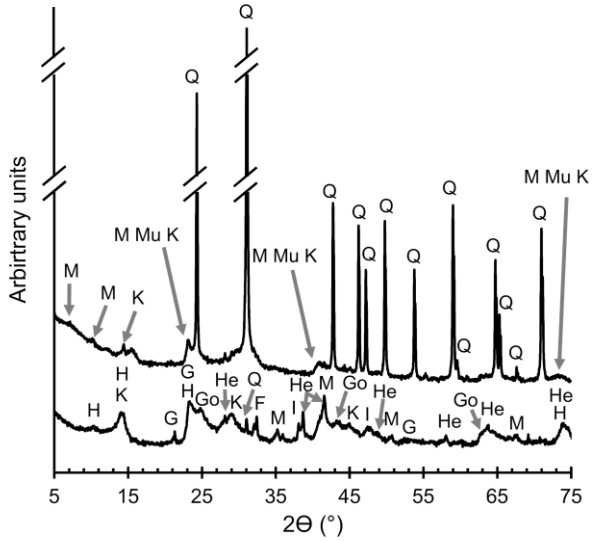

Figure 5: X-ray diffractogram (λ=1.789 Å) of the Nitisol (bottom) and Arenosol (top) with mineral phase identification (M: montmorillonite; Mu: muscovite; K: kaolinite; Q: quartz; H: halloysite; G: gibbsite; M: magnetite/maghemite; I: ilmenite; He: hematite; Go: goethite; F: feldspar).

References

(1) Le Bars, M.; Legros, S.; Levard, C.; Chaurand, P.; Tella, M.; Rovezzi, M.; Browne, P.; Rose, J.; Doelsch, E. Drastic Change in Zinc Speciation during Anaerobic Digestion and Composting: Instability of Nanosized Zinc Sulfide. *Environ. Sci. Technol.* **2018**, *52* (22), 12987–12996. https://doi.org/10.1021/acs.est.8b02697.

(2) Alburquerque, J. A.; de la Fuente, C.; Ferrer-Costa, A.; Carrasco, L.; Cegarra, J.; Abad, M.; Bernal, M. P. Assessment of the Fertiliser Potential of Digestates from Farm and Agroindustrial

Residues. *Biomass Bioenergy* **2012**, *40*, 181–189. https://doi.org/10.1016/j.biombioe.2012.02.018.
(3) Zirkler, D.; Peters, A.; Kaupenjohann, M. Elemental Composition of Biogas Residues: Variability and Alteration during Anaerobic Digestion. *Biomass Bioenergy* **2014**, *67*, 89–98. https://doi.org/10.1016/j.biombioe.2014.04.021.
(4) Romeo, A.; Vacchina, V.; Legros, S.; Doelsch, E. Zinc Fate in Animal Husbandry Systems. *Metallomics* **2014**, *6* (11), 1999–2009. https://doi.org/10.1039/c4mt00062e.
(5) Alvarenga, P.; Mourinha, C.; Farto, M.; Santos, T.; Palma, P.; Sengo, J.; Morais, M.-C.; Cunha-Queda, C. Sewage Sludge, Compost and Other Representative Organic Wastes as Agricultural Soil Amendments: Benefits versus Limiting Factors. *Waste Manag.* **2015**, *40*, 44–52. https://doi.org/10.1016/j.wasman.2015.01.027.
(6) Tella, M.; Doelsch, E.; Letourmy, P.; Chataing, S.; Cuoq, F.; Bravin, M. N.; Saint Macary, H. Investigation of Potentially Toxic Heavy Metals in Different Organic Wastes Used to Fertilize Market Garden Crops. *Waste Manag.* **2013**, *33* (1), 184–192. https://doi.org/10.1016/j.wasman.2012.07.021.
(7) Gottschalk, F.; Sonderer, T.; Scholz, R. W.; Nowack, B. Modeled Environmental Concentrations of Engineered Nanomaterials (TiO2, ZnO, Ag, CNT, Fullerenes) for Different Regions. *Environ. Sci. Technol.* **2009**, *43* (24), 9216–9222. https://doi.org/10.1021/es9015553.
(8) Lombi, E.; Donner, E.; Tavakkoli, E.; Turney, T. W.; Naidu, R.; Miller, B. W.; Scheckel, K. G. Fate of Zinc Oxide Nanoparticles during Anaerobic Digestion of Wastewater and Post-Treatment Processing of Sewage Sludge. *Environ. Sci. Technol.* **2012**, *46* (16), 9089–9096. https://doi.org/10.1021/es301487s.
(9) Ma, R.; Levard, C.; Judy, J. D.; Unrine, J. M.; Durenkamp, M.; Martin, B.; Jefferson, B.; Lowry, G. V. Fate of Zinc Oxide and Silver Nanoparticles in a Pilot Wastewater Treatment Plant and in Processed Biosolids. *Environ. Sci. Technol.* **2014**, *48* (1), 104–112. https://doi.org/10.1021/es403646x.
(10) Nowack, B.; Bucheli, T. D. Occurrence, Behavior and Effects of Nanoparticles in the Environment. *Environ. Pollut.* **2007**, *150* (1), 5–22. https://doi.org/10.1016/j.envpol.2007.06.006.
(11) Cornelis, G.; Hund-Rinke, K.; Kuhlbusch, T.; van den Brink, N.; Nickel, C. Fate and Bioavailability of Engineered Nanoparticles in Soils: A Review. *Crit. Rev. Environ. Sci. Technol.* **2014**, *44* (24), 2720–2764. https://doi.org/10.1080/10643389.2013.829767.
(12) Lead, J. R.; Batley, G. E.; Alvarez, P. J. J.; Croteau, M.-N.; Handy, R. D.; McLaughlin, M. J.; Judy, J. D.; Schirmer, K. Nanomaterials in the Environment: Behavior, Fate, Bioavailability, and Effects—An Updated Review. *Environ. Toxicol. Chem.* **2018**, *37* (8), 2029–2063. https://doi.org/10.1002/etc.4147.
(13) Desmau, M.; Carboni, A.; Le Bars, M.; Doelsch, E.; Benedetti, M. F.; Auffan, M.; Levard, C.; Gelabert, A. How Microbial Biofilms Control the Environmental Fate of Engineered Nanoparticles? *Front. Environ. Sci.* **2020**, *8*, 82. https://doi.org/10.3389/fenvs.2020.00082.
(14) Oleszczuk, P.; Czech, B.; Kończak, M.; Bogusz, A.; Siatecka, A.; Godlewska, P.; Wiesner, M. Impact of ZnO and ZnS Nanoparticles in Sewage Sludge-Amended Soil on Bacteria, Plant and Invertebrates. *Chemosphere* **2019**, *237*, 124359. https://doi.org/10.1016/j.chemosphere.2019.124359.
(15) Bao, S.; Huang, M.; Tang, W.; Wang, T.; Xu, J.; Fang, T. Opposite Effects of the Earthworm Eisenia Fetida on the Bioavailability of Zn in Soils Amended with ZnO and ZnS Nanoparticles. *Environ. Pollut.* **2020**, *260*, 114045. https://doi.org/10.1016/j.envpol.2020.114045.
(16) Chen, C.; Unrine, J. M.; Hu, Y.; Guo, L.; Tsyusko, O. V.; Fan, Z.; Liu, S.; Wei, G. Responses of Soil Bacteria and Fungal Communities to Pristine and Sulfidized Zinc Oxide Nanoparticles Relative to Zn Ions. *J. Hazard. Mater.* **2021**, *405*, 124258. https://doi.org/10.1016/j.jhazmat.2020.124258.

(17) Auffan, M.; Rose, J.; Wiesner, M. R.; Bottero, J.-Y. Chemical Stability of Metallic Nanoparticles: A Parameter Controlling Their Potential Cellular Toxicity in Vitro. *Environ. Pollut.* **2009**, *157* (4), 1127–1133. https://doi.org/10.1016/j.envpol.2008.10.002.

(18) Naidu, R.; Semple, K. T.; Megharaj, M.; Juhasz, A. L.; Bolan, N. S.; Gupta, S. K.; Clothier, B. E.; Schulin, R. Chapter 3 Bioavailability: Definition, Assessment and Implications for Risk Assessment. In *Developments in Soil Science*; Hartemink, A. E., McBratney, A. B., Naidu, R., Eds.; Elsevier: Amsterdam, The Netherlands, 2008; Vol. 32, pp 39–51. https://doi.org/10.1016/S0166-2481(07)32003-5.

(19) Auffan, M.; Rose, J.; Bottero, J.-Y.; Lowry, G. V.; Jolivet, J.-P.; Wiesner, M. R. Towards a Definition of Inorganic Nanoparticles from an Environmental, Health and Safety Perspective. *Nat. Nanotechnol.* **2009**, *4* (10), 634–641. https://doi.org/10.1038/nnano.2009.242.

(20) Mudunkotuwa, I. A.; Grassian, V. H. The Devil Is in the Details (or the Surface): Impact of Surface Structure and Surface Energetics on Understanding the Behavior of Nanomaterials in the Environment. *J. Environ. Monit.* **2011**, *13* (5), 1135–1144. https://doi.org/10.1039/C1EM00002K.

(21) Kim, B.; Levard, C.; Murayama, M.; Brown Jr., G. E.; Hochella Jr., M. F. Integrated Approaches of X-Ray Absorption Spectroscopic and Electron Microscopic Techniques on Zinc Speciation and Characterization in a Final Sewage Sludge Product. *J. Environ. Qual.* **2014**, *43* (3), 908–916. https://doi.org/10.2134/jeq2013.10.0418.

(22) Legros, S.; Levard, C.; Marcato-Romain, C.-E.; Guiresse, M.; Doelsch, E. Anaerobic Digestion Alters Copper and Zinc Speciation. *Environ. Sci. Technol.* **2017**, *51* (18), 10326–10334. https://doi.org/10.1021/acs.est.7b01662.

(23) Formentini, T. A.; Legros, S.; Fernandes, C. V. S.; Pinheiro, A.; Le Bars, M.; Levard, C.; Mallmann, F. J. K.; da Veiga, M.; Doelsch, E. Radical Change of Zn Speciation in Pig Slurry Amended Soil: Key Role of Nano-Sized Sulfide Particles. *Environ. Pollut.* **2017**, *222*, 495–503. https://doi.org/10.1016/j.envpol.2016.11.056.

(24) Voegelin, A.; Jacquat, O.; Pfister, S.; Barmettler, K.; Scheinost, A. C.; Kretzschmar, R. Time-Dependent Changes of Zinc Speciation in Four Soils Contaminated with Zincite or Sphalerite. *Environ. Sci. Technol.* **2011**, *45* (1), 255–261. https://doi.org/10.1021/es101189d.

(25) Scheinost, A. C.; Kretzschmar, R.; Pfister, S.; Roberts, D. R. Combining Selective Sequential Extractions, X-Ray Absorption Spectroscopy, and Principal Component Analysis for Quantitative Zinc Speciation in Soil. *Environ. Sci. Technol.* **2002**, *36* (23), 5021–5028. https://doi.org/10.1021/es025669f.

(26) Manceau, A.; Marcus, M. A.; Tamura, N.; Proux, O.; Geoffroy, N.; Lanson, B. Natural Speciation of Zn at the Micrometer Scale in a Clayey Soil Using X-Ray Fluorescence, Absorption, and Diffraction. *Geochim. Cosmochim. Acta* **2004**, *68* (11), 2467–2483. https://doi.org/10.1016/j.gca.2003.11.021.

(27) Rieuwerts, J. S. The Mobility and Bioavailability of Trace Metals in Tropical Soils: A Review. *Chem. Speciat. Bioavailab.* **2007**, *19* (2), 75–85. https://doi.org/10.3184/095422907X211918.

(28) Kumpiene, J.; Lagerkvist, A.; Maurice, C. Stabilization of As, Cr, Cu, Pb and Zn in Soil Using Amendments – A Review. *Waste Manag.* **2008**, *28* (1), 215–225. https://doi.org/10.1016/j.wasman.2006.12.012.

(29) Sipos, P.; Németh, T.; Kis, V. K.; Mohai, I. Sorption of Copper, Zinc and Lead on Soil Mineral Phases. *Chemosphere* **2008**, *73* (4), 461–469. https://doi.org/10.1016/j.chemosphere.2008.06.046.

(30) Doelsch, E.; Masion, A.; Moussard, G.; Chevassus-Rosset, C.; Wojciechowicz, O. Impact of Pig Slurry and Green Waste Compost Application on Heavy Metal Exchangeable Fractions in Tropical Soils. *Geoderma* **2010**, *155* (3), 390–400. https://doi.org/10.1016/j.geoderma.2009.12.024.

(31) Birks, L. S.; Friedman, H. Particle Size Determination from X-Ray Line Broadening. *J. Appl. Phys.* **1946**, *17* (8), 687–692. https://doi.org/10.1063/1.1707771.

(32) Tella, M.; Bravin, M. N.; Thuriès, L.; Cazevieille, P.; Chevassus-Rosset, C.; Collin, B.; Chaurand, P.; Legros, S.; Doelsch, E. Increased Zinc and Copper Availability in Organic Waste Amended Soil Potentially Involving Distinct Release Mechanisms. *Environ. Pollut.* **2016**, *212*, 299–306. https://doi.org/10.1016/j.envpol.2016.01.077.

(33) Al-Wabel, M. I.; Usman, A. R. A.; Al-Farraj, A. S.; Ok, Y. S.; Abduljabbar, A.; Al-Faraj, A. I.; Sallam, A. S. Date Palm Waste Biochars Alter a Soil Respiration, Microbial Biomass Carbon, and Heavy Metal Mobility in Contaminated Mined Soil. *Environ. Geochem. Health* **2019**, *41* (4), 1705–1722. https://doi.org/10.1007/s10653-017-9955-0.

(34) Tapia, Y.; Cala, V.; Eymar, E.; Frutos, I.; Gárate, A.; Masaguer, A. Chemical Characterization and Evaluation of Composts as Organic Amendments for Immobilizing Cadmium. *Bioresour. Technol.* **2010**, *101* (14), 5437–5443. https://doi.org/10.1016/j.biortech.2010.02.034.

(35) Watson, C.; Schlösser, C.; Vögerl, J.; Wichern, F. Hydrochar, Digestate, and Process Water Impacts on a Soil's Microbial Community, Processes, and Metal Bioavailability. *Soil Sci. Soc. Am. J.* **2021**, *85* (3), 717–731. https://doi.org/10.1002/saj2.20239.

(36) Degryse, F.; Smolders, E.; Oliver, I.; Zhang, H. Relating Soil Solution Zn Concentration to Diffusive Gradients in Thin Films Measurements in Contaminated Soils. *Environ. Sci. Technol.* **2003**, *37* (17), 3958–3965. https://doi.org/10.1021/es034075p.

(37) Zhang, H.; Davison, W.; Knight, B.; McGrath, S. In Situ Measurements of Solution Concentrations and Fluxes of Trace Metals in Soils Using DGT. **1998**. https://doi.org/10.1021/es9704388.

(38) Mason, S.; McNeill, A.; McLaughlin, M. J.; Zhang, H. Prediction of Wheat Response to an Application of Phosphorus under Field Conditions Using Diffusive Gradients in Thin-Films (DGT) and Extraction Methods. *Plant Soil* **2010**, *337* (1), 243–258. https://doi.org/10.1007/s11104-010-0521-0.

(39) Tandy, S.; Mundus, S.; Yngvesson, J.; de Bang, T. C.; Lombi, E.; Schjoerring, J. K.; Husted, S. The Use of DGT for Prediction of Plant Available Copper, Zinc and Phosphorus in Agricultural Soils. *Plant Soil* **2011**, *346* (1), 167–180. https://doi.org/10.1007/s11104-011-0806-y.

(40) Zhang, H.; Zhao, F.-J.; Sun, B.; Davison, W.; Mcgrath, S. P. A New Method to Measure Effective Soil Solution Concentration Predicts Copper Availability to Plants. *Environ. Sci. Technol.* **2001**, *35* (12), 2602–2607. https://doi.org/10.1021/es000268q.

(41) Sekine, R.; Brunetti, G.; Donner, E.; Khaksar, M.; Vasilev, K.; Jämting, Å. K.; Scheckel, K. G.; Kappen, P.; Zhang, H.; Lombi, E. Speciation and Lability of Ag-, AgCl-, and Ag2S-Nanoparticles in Soil Determined by X-Ray Absorption Spectroscopy and Diffusive Gradients in Thin Films. *Environ. Sci. Technol.* **2015**, *49* (2), 897–905. https://doi.org/10.1021/es504229h.

(42) Pouran, H. M.; Martin, F. L.; Zhang, H. Measurement of ZnO Nanoparticles Using Diffusive Gradients in Thin Films: Binding and Diffusional Characteristics. *Anal. Chem.* **2014**, *86* (12), 5906–5913. https://doi.org/10.1021/ac500730s.

(43) Ravel, B.; Newville, M. ATHENA, ARTEMIS, HEPHAESTUS: Data Analysis for X-Ray Absorption Spectroscopy Using IFEFFIT. *J. Synchrotron Radiat.* **2005**, *12* (4), 537–541. https://doi.org/10.1107/S0909049505012719.

(44) Rose, J.; Moulin, I.; Masion, A.; Bertsch, P. M.; Wiesner, M. R.; Bottero, J.-Y.; Mosnier, F.; Haehnel, C. X-Ray Absorption Spectroscopy Study of Immobilization Processes for Heavy Metals in Calcium Silicate Hydrates. 2. Zinc. *Langmuir* **2001**, *17* (12), 3658–3665. https://doi.org/10.1021/la001302h.

(45) Pokrovsky, O. S.; Pokrovski, G. S.; Gélabert, A.; Schott, J.; Boudou, A. Speciation of Zn Associated with Diatoms Using X-Ray Absorption Spectroscopy. *Environ. Sci. Technol.* **2005**, *39* (12), 4490–4498. https://doi.org/10.1021/es0480419.

(46) Hammer, D.; Keller, C.; McLaughlin, M. J.; Hamon, R. E. Fixation of Metals in Soil Constituents and Potential Remobilization by Hyperaccumulating and Non-Hyperaccumulating Plants: Results from an Isotopic Dilution Study. *Environ. Pollut.* **2006**, *143* (3), 407–415. https://doi.org/10.1016/j.envpol.2005.12.008.

(47) Sammut, M. L.; Rose, J.; Masion, A.; Fiani, E.; Depoux, M.; Ziebel, A.; Hazemann, J. L.; Proux, O.; Borschneck, D.; Noack, Y. Determination of Zinc Speciation in Basic Oxygen Furnace Flying Dust by Chemical Extractions and X-Ray Spectroscopy. *Chemosphere* **2008**, *70* (11), 1945–1951. https://doi.org/10.1016/j.chemosphere.2007.09.063.
(48) Phan, H. T.; Haes, A. J. What Does Nanoparticle Stability Mean? *J. Phys. Chem. C* **2019**, *123* (27), 16495–16507. https://doi.org/10.1021/acs.jpcc.9b00913.
(49) Robson, T. C.; Braungardt, C. B.; Rieuwerts, J.; Worsfold, P. Cadmium Contamination of Agricultural Soils and Crops Resulting from Sphalerite Weathering. *Environ. Pollut.* **2014**, *184*, 283–289. https://doi.org/10.1016/j.envpol.2013.09.001.
(50) Gilbert, B.; Huang, F.; Zhang, H.; Waychunas, G. A.; Banfield, J. F. Nanoparticles: Strained and Stiff. *Science* **2004**, *305* (5684), 651–654. https://doi.org/10.1126/science.1098454.
(51) Huang, Z.; Thomson, P.; Di, S. Lattice Contractions of a Nanoparticle Due to the Surface Tension: A Model of Elasticity. *J. Phys. Chem. Solids* **2007**, *68* (4), 530–535. https://doi.org/10.1016/j.jpcs.2007.01.016.
(52) Degryse, F.; Smolders, E.; Parker, D. R. Partitioning of Metals (Cd, Co, Cu, Ni, Pb, Zn) in Soils: Concepts, Methodologies, Prediction and Applications – a Review. *Eur. J. Soil Sci.* **2009**. https://doi.org/10.1111/j.1365-2389.2009.01142.x.
(53) Siy, J. T.; Bartl, M. H. Insights into Reversible Dissolution of Colloidal CdSe Nanocrystal Quantum Dots. *Chem. Mater.* **2010**, *22* (21), 5973–5982. https://doi.org/10.1021/cm102156v.
(54) Chappell, M. A.; Miller, L. F.; George, A. J.; Pettway, B. A.; Price, C. L.; Porter, B. E.; Bednar, A. J.; Seiter, J. M.; Kennedy, A. J.; Steevens, J. A. Simultaneous Dispersion–Dissolution Behavior of Concentrated Silver Nanoparticle Suspensions in the Presence of Model Organic Solutes. *Chemosphere* **2011**, *84* (8), 1108–1116. https://doi.org/10.1016/j.chemosphere.2011.04.040.
(55) Ravichandran, M.; Aiken, G. R.; Reddy, M. M.; Ryan, J. N. Enhanced Dissolution of Cinnabar (Mercuric Sulfide) by Dissolved Organic Matter Isolated from the Florida Everglades. *Environ. Sci. Technol.* **1998**, *32* (21), 3305–3311. https://doi.org/10.1021/es9804058.
(56) Waples, J. S.; Nagy, K. L.; Aiken, G. R.; Ryan, J. N. Dissolution of Cinnabar (HgS) in the Presence of Natural Organic Matter. *Geochim. Cosmochim. Acta* **2005**, *69* (6), 1575–1588. https://doi.org/10.1016/j.gca.2004.09.029.
(57) Hoffmann, K.; Bouchet, S.; Christl, I.; Kaegi, R.; Kretzschmar, R. Effect of NOM on Copper Sulfide Nanoparticle Growth, Stability, and Oxidative Dissolution. *Environ. Sci. Nano* **2020**, *7* (4), 1163–1178. https://doi.org/10.1039/C9EN01448A.
(58) Zhang, H.; Chen, B.; Banfield, J. F. Particle Size and PH Effects on Nanoparticle Dissolution. *J. Phys. Chem. C* **2010**, *114* (35), 14876–14884. https://doi.org/10.1021/jp1060842.
(59) Cheng, T.; Allen, H. E. Comparison of Zinc Complexation Properties of Dissolved Natural Organic Matter from Different Surface Waters. *J. Environ. Manage.* **2006**, *80* (3), 222–229. https://doi.org/10.1016/j.jenvman.2005.09.007.
(60) Heidel, C.; Tichomirowa, M.; Breitkopf, C. Sphalerite Oxidation Pathways Detected by Oxygen and Sulfur Isotope Studies. *Appl. Geochem.* **2011**, *26* (12), 2247–2259. https://doi.org/10.1016/j.apgeochem.2011.08.007.
(61) Rimstidt, J. D.; Chermak, J. A.; Gagen, P. M. Rates of Reaction of Galena, Sphalerite, Chalcopyrite, and Arsenopyrite with Fe(III) in Acidic Solutions. In *Environmental Geochemistry of Sulfide Oxidation*; Alpers, C. N., Blowes, D. W., Eds. ; ACS Symposium Series; American Chemical Society, 1993; Vol. 550, pp 2–13. https://doi.org/10.1021/bk-1994-0550.ch001.
(62) Fowler, T. A.; Crundwell, F. K. Leaching of Zinc Sulfide by Thiobacillus Ferrooxidans: Bacterial Oxidation of the Sulfur Product Layer Increases the Rate of Zinc Sulfide Dissolution at High Concentrations of Ferrous Ions. *Appl. Environ. Microbiol.* **1999**, *65* (12), 5285–5292.
(63) Lors, C.; Tiffreau, C.; Laboudigue, A. Effects of Bacterial Activities on the Release of Heavy Metals from Contaminated Dredged Sediments. *Chemosphere* **2004**, *56* (6), 619–630. https://doi.org/10.1016/j.chemosphere.2004.04.009.
(64) Chapman, S. J. Thiobacillus Populations in Some Agricultural Soils. *Soil Biol. Biochem.* **1990**, *22* (4), 479–482. https://doi.org/10.1016/0038-0717(90)90181-X.

(65) Tourna, M.; Maclean, P.; Condron, L.; O'Callaghan, M.; Wakelin, S. A. Links between Sulphur Oxidation and Sulphur-Oxidising Bacteria Abundance and Diversity in Soil Microcosms Based on SoxB Functional Gene Analysis. *FEMS Microbiol. Ecol.* **2014**, *88* (3), 538–549. https://doi.org/10.1111/1574-6941.12323.
(66) Pokorna, D.; Zabranska, J. Sulfur-Oxidizing Bacteria in Environmental Technology. *Biotechnol. Adv.* **2015**, *33* (6, Part 2), 1246–1259. https://doi.org/10.1016/j.biotechadv.2015.02.007.
(67) Desmau, M.; Levard, C.; Vidal, V.; Ona-Nguema, G.; Charron, G.; Benedetti, M. F.; Gélabert, A. How Microbial Biofilms Impact the Interactions of Quantum Dots with Mineral Surfaces? *NanoImpact* **2020**, *19*, 100247. https://doi.org/10.1016/j.impact.2020.100247.
(68) Evans, L. J. Chemistry of Metal Retention by Soils. *Environ. Sci. Technol.* **1989**, *23* (9), 1046–1056. https://doi.org/10.1021/es00067a001.
(69) Rieuwerts, J. ; Thornton, I.; Farago, M. ; Ashmore, M. Factors Influencing Metal Bioavailability in Soils: Preliminary Investigations for the Development of a Critical Loads Approach for Metals. *Chem. Speciat. Bioavailab.* **1998**, *10* (2), 61–75. https://doi.org/10.3184/095422998782775835.
(70) Sauvé, S.; Hendershot, W.; Allen, H. E. Solid-Solution Partitioning of Metals in Contaminated Soils: Dependence on PH, Total Metal Burden, and Organic Matter. *Environ. Sci. Technol.* **2000**, *34* (7), 1125–1131. https://doi.org/10.1021/es9907764.
(71) Foth, H. D. *Fundamentals of Soil Science*, 8th edition.; Wiley: New York, 1978.
(72) Rutkowska, B.; Szulc, W.; Bomze, K.; Gozdowski, D.; Spychaj-Fabisiak, E. Soil Factors Affecting Solubility and Mobility of Zinc in Contaminated Soils. *Int. J. Environ. Sci. Technol.* **2014**. https://doi.org/10.1007/s13762-014-0546-7.
(73) Ha, J.; Farges, F.; Brown, G. E. Adsorption and Precipitation of Aqueous Zn(II) on Hematite Nano- and Microparticles. In *AIP Conference Proceedings;* Stanford, California (USA), **2007**, Vol. 882, pp 238–240.
(74) Nachtegaal, M.; Sparks, D. L. Effect of Iron Oxide Coatings on Zinc Sorption Mechanisms at the Clay-Mineral/Water Interface. *J. Colloid Interface Sci.* **2004**, *276* (1), 13–23. https://doi.org/10.1016/j.jcis.2004.03.031.
(75) Stietiya, M. H.; Wang, J. J.; Roy, A. Macroscopic and Extended X-Ray Absorption Fine Structure Spectroscopic Investigation of Ligand Effect on Zinc Adsorption to Kaolinite as a Function of PH. *Soil Sci.* **2011**, *176* (9), 464–471. https://doi.org/10.1097/SS.0b013e3182285b46.
(76) Nelson, J.; Wasylenki, L.; Bargar, J. R.; Brown, G. E.; Maher, K. Effects of Surface Structural Disorder and Surface Coverage on Isotopic Fractionation during Zn(II) Adsorption onto Quartz and Amorphous Silica Surfaces. *Geochim. Cosmochim. Acta* **2017**, *215*, 354–376. https://doi.org/10.1016/j.gca.2017.08.003.
(77) Xia, K.; Bleam, W.; Helmke, P. A. Studies of the Nature of Binding Sites of First Row Transition Elements Bound to Aquatic and Soil Humic Substances Using X-Ray Absorption Spectroscopy. *Geochim. Cosmochim. Acta* **1997**, *61* (11), 2223–2235. https://doi.org/10.1016/S0016-7037(97)00080-X.
(78) Sarret, G.; Manceau, A.; Hazemann, J. L.; Gomez, A.; Mench, M. EXAFS Study of the Nature of Zinc Complexation Sites in Humic Substances as a Function of Zn Concentration. *J. Phys. IV* **1997**, *7* (C2), C2-C2-802. https://doi.org/10.1051/jp4:1997239.
(79) Karlsson, T.; Skyllberg, U. Complexation of Zinc in Organic Soils - EXAFS Evidence for Sulfur Associations. *Environ. Sci. Technol.* **2007**, *41* (1), 119–124. https://doi.org/10.1021/es0608803.
(80) Hooda, P. S.; Zhang, H.; Davison, W.; Edwards, A. C. Measuring Bioavailable Trace Metals by Diffusive Gradients in Thin Films (DGT): Soil Moisture Effects on Its Performance in Soils. *Eur. J. Soil Sci.* **1999**, *50* (2), 285–294. https://doi.org/10.1046/j.1365-2389.1999.00226.x.
(81) Hamamoto, S.; Perera, M. S. A.; Resurreccion, A.; Kawamoto, K.; Hasegawa, S.; Komatsu, T.; Moldrup, P. The Solute Diffusion Coefficient in Variably Compacted, Unsaturated Volcanic Ash Soils. *Vadose Zone J.* **2009**, *8* (4), 942–952. https://doi.org/https://doi.org/10.2136/vzj2008.0184.

(82) Olesen, T.; Moldrup, P.; Gamst, J. Solute Diffusion and Adsorption in Six Soils along a Soil Texture Gradient. *Soil Sci. Soc. Am. J.* **1999**, *63* (3), 519–524. https://doi.org/10.2136/sssaj1999.03615995006300030014x.
(83) Olesen, T.; Moldrup, P.; Yamaguchi, T.; Rolston, D. E. Constant Slope Impedance Factor Model for Predicting the Solute Diffusion Coefficient in Unsaturated Soil. *Soil Sci.* **2001**, *166* (2), 89–96.
(84) Moldrup, P.; Olesen, T.; Blendstrup, H.; Komatsu, T.; de Jonge, L. W.; Rolston, D. E. Predictive-Descriptive Models for Gas and Solute Diffusion Coefficients in Variably Saturated Porous Media Coupled to Pore-Size Distribution: IV. Solute Diffusivity and the Liquid Phase Impedance Factor. *Soil Sci.* **2007**, *170 (111), 854-866.*
(85) Moreau, J. W.; Weber, P. K.; Martin, M. C.; Gilbert, B.; Hutcheon, I. D.; Banfield, J. F. Extracellular Proteins Limit the Dispersal of Biogenic Nanoparticles. *Science* **2007**, *316* (5831), 1600–1603. https://doi.org/10.1126/science.1141064.
(86) Lau, B. L. T.; Hsu-Kim, H. Precipitation and Growth of Zinc Sulfide Nanoparticles in the Presence of Thiol-Containing Natural Organic Ligands. *Environ. Sci. Technol.* **2008**, *42* (19), 7236–7241. https://doi.org/10.1021/es801360b.
(87) Gondikas, A. P.; Masion, A.; Auffan, M.; Lau, B. L. T.; Hsu-Kim, H. Early-Stage Precipitation Kinetics of Zinc Sulfide Nanoclusters Forming in the Presence of Cysteine. *Chem. Geol.* **2012**, *329*, 10–17. https://doi.org/10.1016/j.chemgeo.2011.06.009.
(88) Zhang, H.; Gilbert, B.; Huang, F.; Banfield, J. F. Water-Driven Structure Transformation in Nanoparticles at Room Temperature. *Nature* **2003**, *424* (6952), 1025–1029. https://doi.org/10.1038/nature01845.
(89) Panfili, F.; Manceau, A.; Sarret, G.; Spadini, L.; Kirpichtchikova, T.; Bert, V.; Laboudigue, A.; Marcus, M. A.; Ahamdach, N.; Libert, M.-F. The Effect of Phytostabilization on Zn Speciation in a Dredged Contaminated Sediment Using Scanning Electron Microscopy, X-Ray Fluorescence, EXAFS Spectroscopy, and Principal Components Analysis. *Geochim. Cosmochim. Acta* **2005**, *69* (9), 2265–2284. https://doi.org/10.1016/j.gca.2004.10.017.
(90) Hodomihou, N. R.; Feder, F.; Legros, S.; Formentini, T. A.; Lombi, E.; Doelsch, E. Zinc Speciation in Organic Waste Drives Its Fate in Amended Soils. *Environ. Sci. Technol.* **2020**, *54* (19), 12034–12041. https://doi.org/10.1021/acs.est.0c02721.